



Unsupervised Clustering Methods for Lung Perfusion Data Segmentation in Electrical Impedance Tomography

Arthur Ribeiro, Yu Xia, Monica Matsumoto and Marcus Victor

EasyChair preprints are intended for rapid dissemination of research results and are integrated with the rest of EasyChair.

January 29, 2025

Unsupervised clustering methods for lung perfusion data segmentation in electrical impedance tomography

A. S. Ribeiro¹, Y. H. W. Xia², M. M. S. Matsumoto² and M. H. Victor Jr²

¹ Institute of Science and Technology - ICT, Federal University of São Paulo - UNIFESP, São José dos Campos, Brazil.

² Electronics Engineering Division, Aeronautics Institute of Technology - ITA, São José dos Campos, São Paulo, Brazil

Abstract— In this work, we evaluated unsupervised clustering methods in segmenting the electrical impedance tomography image during the assessment of pulmonary perfusion by injection of hypertonic saline solution. In clustering the image pixels, we assume the existence of purely lung pixels (solely due to lung perfusion without effects from other organs) and hybrid pixels (which contain heart and lung effects together). We used data from 5 pigs to generate truth masks and assess the quality of clustering. Among the methods tested, the k-means with the cosine metric proved to be the best, as it obtained the 95% sensitivity median and the 90% specificity median. We prioritized minimizing the false negative cases and false positive cases, as it would overestimate regional pulmonary perfusion.

Keywords— electrical impedance tomography, lung perfusion, clustering, k-means, hierarchical clustering.

I. INTRODUCTION

Electrical impedance tomography (EIT) is a non-invasive, non-ionizing, and functional imaging modality. The EIT machine generates images by mapping biological tissues' electrical characteristics. The technique is primarily used to continuously monitor lung ventilation and perfusion in mechanically ventilated patients [1, 2, 3]. For patients with different ventilation conditions (undergoing surgical procedures or lung diseases), EIT allows adjusting the ventilator settings based on the individual needs [4, 5].

The protocol to estimate lung perfusion begins with injecting a hypertonic saline solution into the right atrium that takes the blood to the lungs. This procedure modifies and decreases the regional impedance [6]. Usually, 16 or 32 electrodes are positioned around the thorax, and a high frequency and low amplitude electrical current is applied for tissue excitation. The electrical potentials are measured and used to calculate the thorax impedance distribution. A reconstruction algorithm uses this data to create the lung perfusion distribution map [7].

The EIT has been verified and validated as a useful method in clinical practice [8, 9], mainly in monitoring lung venti-

lation. The perfusion estimation using EIT has a hindrance caused by the problem of signal interference between lungs and heart where a given voxel captures partial behaviors of the contrast passage through the right heart, the lungs, and returning to the left heart [7, 10]. Some approaches were developed trying to segment the lung and heart regions. These methods include comparing functional EIT images with anatomic images from a computed tomography (CT) slice in the plane of the electrodes. Often, the approaches use unsupervised methods combining statistical and spectral analysis with an image processing algorithm to define the heart and lung regions of interest (ROI) [10].

Another study evaluated whether the EIT could determine the redistribution of lung perfusion elicited by one-lung ventilation. To find the lung and heart ROIs, they applied a Fourier transform to the pixels' time courses of relative impedance change to examine the frequency components of the EIT data. The heart ROI (negative slope) and lung ROI (positive slope) were acquired by calculating the slope of the linear regression fit between the local pixel and global EIT data [11].

This paper proposes a method to segment the EIT image during a hypertonic saline injection to evaluate lung perfusion by clustering the pixels with only lung behavior (solely lung) and pixels with hybrid behavior (heart and lung at the same time). The approaches rely on clustering tools to detect hybrid and lung pixels in the time-series data of five pigs.

II. METHODS

A. Animal experiment

The study relies on landrace swine's experimental data without previous or induced lung injury. The project was approved by the Ethics Committee on the Use of Animals (CEUA) of the Faculty of Medicine of the University of São Paulo (FMUSP) under number 1242/2019. The study was carried out in the animal ICU of the Laboratory of Medical Investigation in Experimental Pulmonology (LIM-09), located on the 4th floor of the FMUSP, and in the Tomography room of the Department of Pathology, located in the basement of the same building.

A belt containing 32 EIT electrodes was positioned in the plane corresponding to the 4th-5th intercostal space on the previously shaved skin. We used the EIT device (Enlight-1800, Timpel, São Paulo, Brazil). For evaluating perfusion by EIT, data were acquired during an apnea period of 30 seconds: 10 seconds pre-injection, followed by a rapid injection of 10 mL of 7.5% NaCl through a central catheter located in the right atrium of the animal. The images obtained by EIT have a sampling rate of 50 Hz and spatial resolution of 32-by-32 pixels in just one slice, representing about 15-20 cm of the lung.

B. Clustering algorithms

We have evaluated two clustering algorithms: k-means and hierarchical clustering. We used the complete dataset to test and assess both methods.

The k-means is an iterative, data-partitioning algorithm that assigns n observations to precisely one of the k clusters. Where k is chosen before the algorithm starts. K-means treats each observation in the data as an object with a space location. The method finds a partition in which objects within each cluster, using a metric distance, are as close to each other as possible. Our experiment used two ($k=2$) clusters: hybrid and lung pixels. We chose the correlation and cosine metric distance based on the pig data signal. An assessment with a metric distance from an origin (cosine and correlation) gives a clustering considering the phase and magnitude between two time series, it is more useful than use the Euclidean metric distance that only find the shortest distance between two time series.

The cosine metric, also called cosine similarity, calculates the cosine of the angle between two points (treated as vectors). The cosine metric distance is shown in Equation 1,

$$d_{cos}(a,b) = 1 - \frac{\sum_{i=1}^n a_i b_i}{\sqrt{\sum_{i=1}^n a_i^2} \sqrt{\sum_{i=1}^n b_i^2}} \quad (1)$$

Where a_i and b_i are the samples of vectors a and b , respectively, n is the number of samples, with the $d_{cos}(a,b)$ as the cosine metric distance between a and b . The cosine metric distance is one minus the cosine similarity and has a range of values between 0 and 2.

The correlation metric distance is shown according to Equations 2, 3 and 4,

$$d_{corr}(a,b) = 1 - \frac{\sum_{i=1}^n (a_i - \bar{a})(b_i - \bar{b})}{\sqrt{\sum_{i=1}^n (a_i - \bar{a})^2} \sqrt{\sum_{i=1}^n (b_i - \bar{b})^2}} \quad (2)$$

$$\bar{a} = \frac{\sum_{i=1}^n a_i}{n} \quad (3)$$

$$\bar{b} = \frac{\sum_{i=1}^n b_i}{n} \quad (4)$$

Where a_i and b_i are samples of a and b respectively, n is the number of samples, with $d_{corr}(a,b)$ as the correlation metric distance between a and b . The correlation metric distance is one minus the correlation and take a range of values from 0 to 2.

The hierarchical clustering method includes grouping data over various scales by creating a cluster tree or dendrogram. The tree is not a single set of clusters but a multilevel hierarchy, where clusters at one level are joined as clusters at the next level. To perform the clustering, the purpose is to find the similarity or dissimilarity between every pair of objects in the data set, calculating the distance between objects. We also used two clusters (hybrid and lung pixels). Based on the pig data signal and to compare k-means and the hierarchical clustering methods, we used the correlation and cosine metric distance in clustering routines [12].

C. Implementation

The dataset consists of each pixel's impedance waveforms per time (samples). The waveforms are shown in Figure 1 (a) and correspond to those pixels that varied during the acquisition. The silent pixels were excluded from the analysis.

During a hypertonic saline injection, the time series of the impedance per time (samples) can be associated with the blood volume, while the time derivative of the impedance per time (samples) is associated with the blood flow. The blood volume does not give quantitative information about how much and what conditions (slow or fast flow) the blood is reaching the lung. Therefore, we decided to analyze only the time derivative waveforms (Figure 1 (b)).

The derivative signals are clustered using k-means and hierarchical clustering with the correlation and cosine metrics. After finishing the clustering step, we reorganized the data in hybrid masks with 32x32 pixels for each derivative result and we apply a morphological operation to dilate and expands the hybrid region. The kernel shape used was "square" with size "2" to increase the true positive pixels and reduce the pixels incorrectly classified.

The result masks were compared with the truth masks (manually created). The method to create the truth masks was observing the EIT derivative signal (32x32 pixels) in time (samples) looking frame by frame and deciding to use the frame that do not presented lung perfusion pixels. The derivative perfusion signal was set with a sequential color scale as

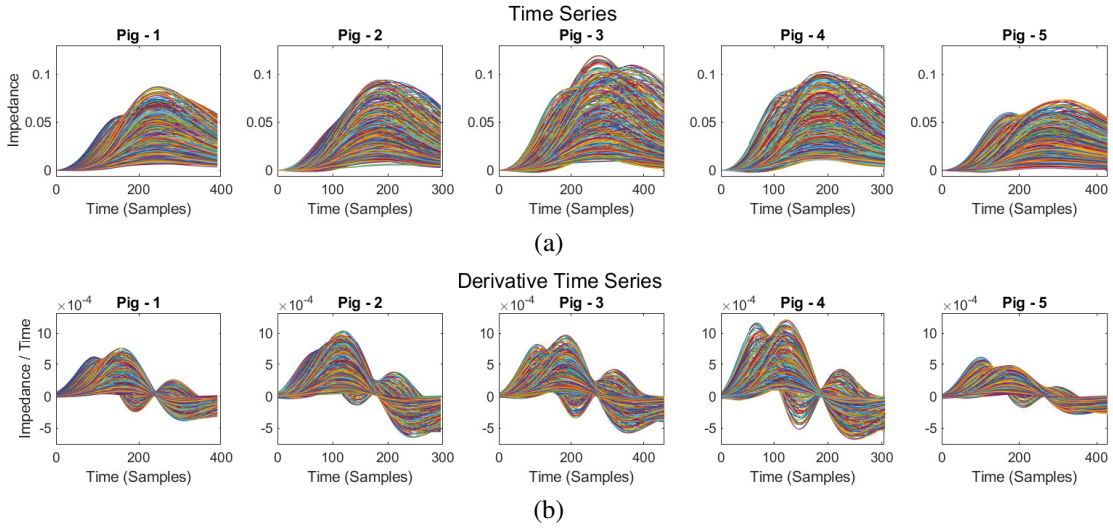


Fig. 1: Time series (a) and derivative (b) for the electrical impedance signal of each pixel.

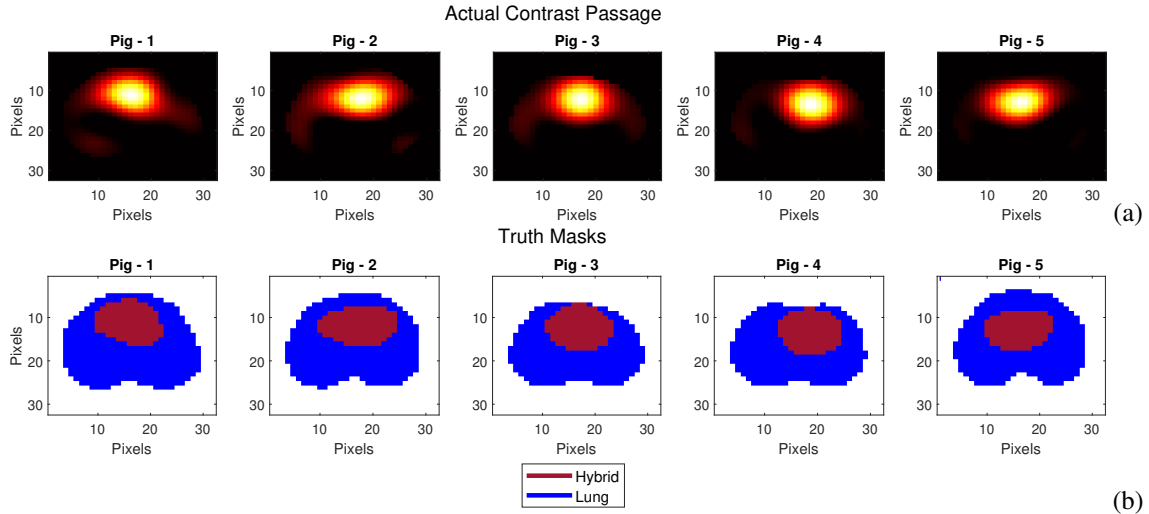


Fig. 2: Actual contrast passage (a) used to create the truth mask (b) with binary colors representing the hybrid and lung regions manually segmented.

shown in Figure 2 (a). The pixels with higher impedance/time present a lighter color. Thus, we selected only the pixels with color $\geq 25\%$ of the chosen scale to the hybrid region (hybrid pixels with considerable signal amplitude), and the others were considered as lung region of the truth mask. The results of the truth masks are visualized in Figure 2 (b).

All hybrid masks comparison results are evaluated quantitatively using the following parameters:

- True Positive (hybrid pixels considered as hybrid pixels);
- True Negative (lung pixels considered as lung pixels);

- False Positive (lung pixels considered as hybrid pixels);
- False Negative (hybrid pixels considered as lung pixels).

The parameters were used to calculate the sensitivity, specificity, and accuracy of each clustering algorithms method.

III. RESULTS

The analysis focus was on the masks comparisons. Each mask was compared with the truth mask (Figure 2 (b)). The

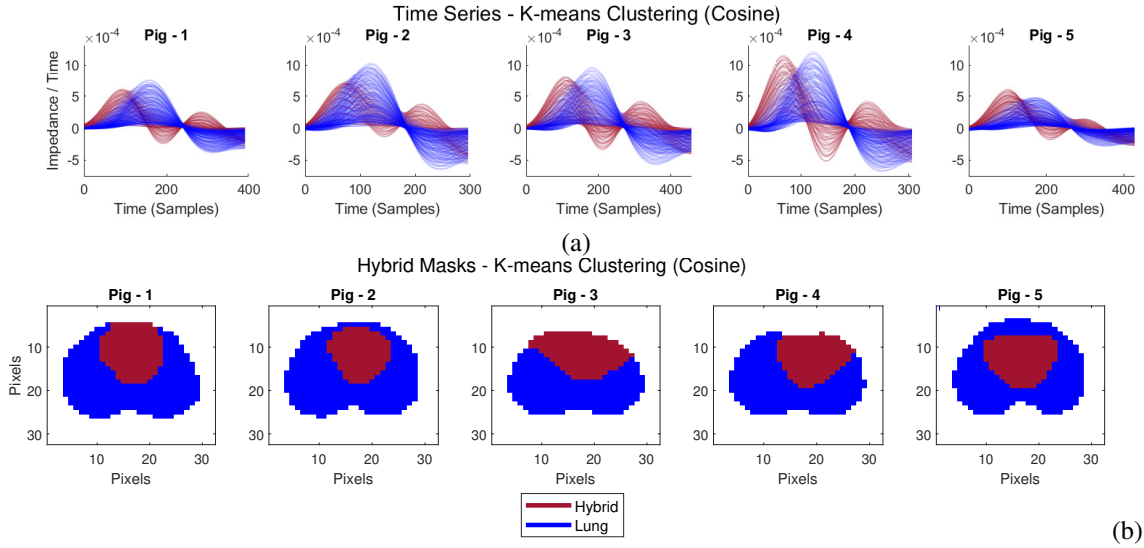


Fig. 3: Time series k-means clustering (Cosine) electrical impedance per samples by each pixel and its Hybrid Mask with K-means Clustering (Cosine); (a) Time series K - means Clustering (Cosine); (b) Hybrid Mask - K - means Clustering (Cosine).

k-means and hierarchical clustering results using the cosine metric are visualized in Tables 1 and 2 respectively. The results using the correlation metric are shown in Tables 3 and 4, respectively.

The tables were used to evaluate which method using each metric quantitatively has shown the best performance. The objective was to examine the higher sensitivity percentage median. The high sensitivity median represents that the method found the higher number of true positive cases (hybrid pixels as actual hybrid pixels) with the lower number of false negative cases (hybrid pixels considered as lung pixels). Evaluating the false negative instead of the false positive is damage control. For the proposed problem, taking a lung pixel as a hybrid pixel is less troublesome than taking a hybrid pixel as a lung pixel.

Table 1: k-means clustering (cosine metric). Sensitivity (TPR) stands for true positive rate; Accuracy (ACC) stands for the accuracy of the method; and Specificity (TNR) stands for true negative rate. All values are in percentage.

Pigs	Sensitivity%	Specificity%	Accuracy %
1	95	90	91
2	83	92	90
3	93	85	87
4	96	90	91
5	98	88	90
Median	95	90	90

Table 2: Hierarchical clustering (cosine metric). Sensitivity (TPR) stands for true positive rate; Accuracy (ACC) stands for the accuracy of the method; and Specificity (TNR) stands for true negative rate. All values are in percentage.

Pigs	Sensitivity %	Specificity%	Accuracy %
1	92	91	91
2	73	95	89
3	89	90	90
4	95	94	94
5	98	89	91
Median	92	91	91

Searching for a method with the higher sensitivity median, we found that the best method was the k-means clustering using the cosine metric, as shown in Table 1. This method presents its clustered time series and masks shown in Figure 3 (a) and 3 (b), respectively. Furthermore, the comparison between the method masks and the truth masks is shown in Figure 4.

IV. DISCUSSIONS

The k-means clustering (cosine metric) has gotten a 95% of sensitivity and 90% of specificity, representing a considerable probability of detection and a high selectivity of the method.

The understanding of the false pixels cases are that the FN

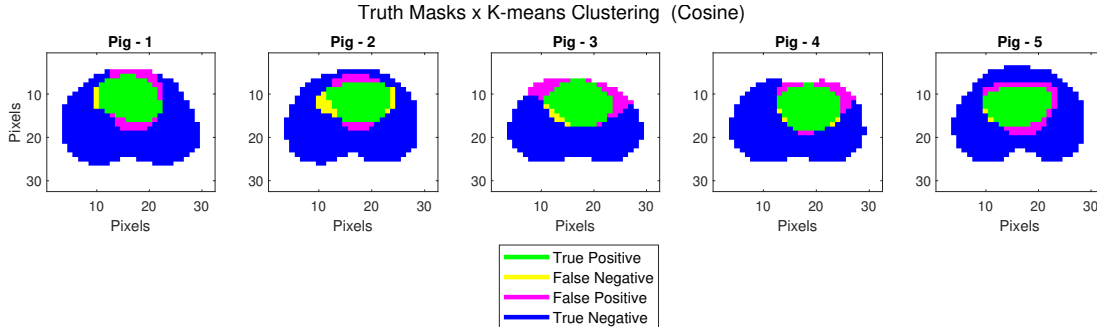


Fig. 4: Comparisons among the truth masks versus k-means clustering (cosine metric) masks.

Table 3: k-means clustering (correlation metric). Sensitivity (TPR) stands for true positive rate; Accuracy (ACC) stands for the accuracy of the method; and Specificity (TNR) stands for true negative rate. All values are in percentage.

Pigs	Sensitivity %	Specificity %	Accuracy %
1	94	89	90
2	73	93	88
3	82	93	90
4	96	89	91
5	98	90	92
Median	94	90	90

Table 4: Hierarchical clustering (correlation metric). Sensitivity (TPR) stands for true positive rate; Accuracy (ACC) stands for the accuracy of the method; and Specificity (TNR) stands for true negative rate. All values are in percentage.

Pigs	Sensitivity %	Specificity %	Accuracy %
1	91	92	92
2	76	94	90
3	88	90	89
4	96	91	92
5	92	94	94
Median	91	92	92

(yellow pixels) means that the hybrid pixels in hybrid mask, has true positive almost all hybrid pixels of the truth mask. However, the FP (pink pixels) reveals some hybrid pixels in hybrid masks should be classified as lung pixels. This implies that the k-means clustering (cosine) finds the true positive with the truth masks hybrid pixels, but it needs to be investigated why some lung pixels are classified as hybrid pixels. Reduce the FP cases is the best way to increase the specificity median.

One approach to investigate what could be interfering in false pixels cases was to plot the clustered time series of this

method (Figure 3 (a)), with the waveforms of FP and FN parameters taken in Figure 4. We show such a plot for this method in Figure 5.

Figure 5 shows essential information about the main errors in our method. We verify that the hybrid pixels and the lung pixels have very different and defined waveforms for each one. Comparing the hybrid and lung pixels peak to the peak of incorrectly classified pixels - FN (yellow pixels) and FP (pink pixels). We observed that the yellow and pink pixels are in an intermediary peak. This information suggests that the intermediary peak influences a wrong hybrid classification by the k-means clustering (cosine).

Furthermore, comparing the pink and yellow waveforms with the lung waveforms, we notice that the similarity (phase and magnitude) between them are higher than the hybrid waveforms. The hybrid waveforms have defined negative region, while the pixels incorrectly classified have not. This information suggests that the cosine metric distance used to create the hybrid masks, has some problems when the waveforms presents a lower similarity.

In synthesis, the method using the k-means clustering (cosine) to create the hybrid masks was the best approach giving a high probability of detection and selectivity, and promising results to be a useful segmentation method to find the hybrid and lung region in a perfusion data set. The main problem is the wrong classification of the lung pixels as hybrid pixels (pink pixels) and to understand the errors, more tests need to be performed.

V. CONCLUSION

This work has shown and compared different methods for waveform clustering in EIT data during lung perfusion assessment. The approaches included using k-means and hierarchical clustering methods using the cosine and correlation metrics. The best result was using the time-derivative dataset waveforms with k-means clustering (cosine metric).

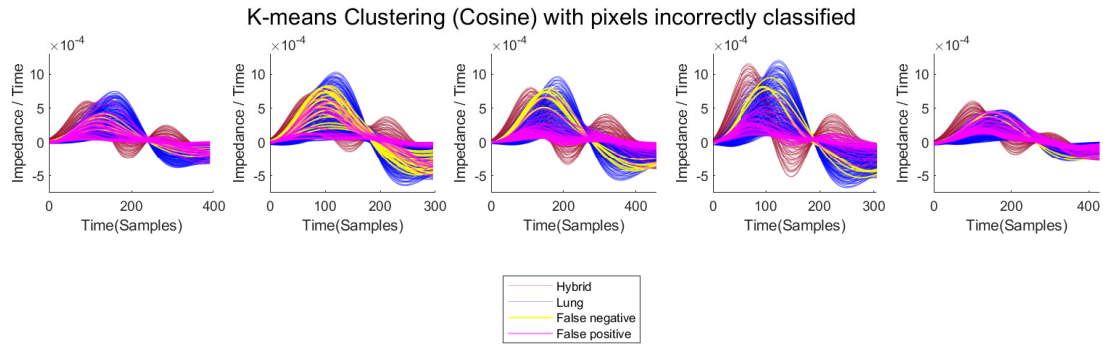


Fig. 5: Time series of k-means clustering (cosine metric) with pixels incorrectly classified (false negative and false positive waveforms) from the comparisons of Figure 4.

This method presents a 95% sensitivity median with a 90% specificity median, highest within the compared methods. The considerable accuracy represents promising results, but more work should be performed to understand the errors between the clustering method and the truth masks.

CONFLICT OF INTEREST

The authors declare that they have no conflict of interest.

ACKNOWLEDGEMENTS

The authors would like to acknowledge the contributions of the funding agency CNPq for the financial support of this research and the Medical Investigations Laboratory (LIM-09) from the Faculty of Medicine of University of São Paulo (FMUSP) for providing the dataset.

REFERENCES

1. Frerichs I, Amato M B P, Kaam A H et al. Chest electrical impedance tomography examination, data analysis, terminology, clinical use and recommendations: consensus statement of the TRanslational EIT developmeNt stuDy group. *Thorax*. 2016;72:83-93.
2. Perier F, Tuffet S, Maraffi T et al. Effect of Positive End-Expiratory Pressure and Proning on Ventilation and Perfusion in COVID-19 Acute Respiratory Distress Syndrome *American Journal of Respiratory and Critical Care Medicine*. 2020;202:1713-1717. PMID: 33075235.
3. Perier F, Tuffet S, Maraffi T et al. Electrical impedance tomography to titrate positive end-expiratory pressure in COVID-19 acute respiratory distress syndrome *Critical Care*. 2020;24:678.

4. Leonhardt S, Pikkemaat R, Stenqvist O et al. Electrical Impedance Tomography for hemodynamic monitoring in *2012 Annual International Conference of the IEEE Engineering in Medicine and Biology Society*:122–125.IEEE 2012.
5. Roldán R, Rodriguez S, Barriga F et al. Sequential lateral positioning as a new lung recruitment maneuver: an exploratory study in early mechanically ventilated Covid-19 ARDS patients 2022;12:13.
6. Brown B H, Leathard A, Sinton A et al. Blood Flow Imaging Using Electrical Impedance Tomography in *Proceedings of the Annual International Conference of the IEEE Engineering in Medicine and Biology Society Volume 13*: 1991:307-308 1991.
7. Costa E L, Lima R G, Amato M B. Electrical impedance tomography. *Curr Opin Crit Care*. 2009;15:18-24.
8. Frerichs I, Hinz J, Herrmann P et al. Regional lung perfusion as determined by electrical impedance tomography in comparison with electron beam CT imaging. *IEEE transactions on medical imaging*. 2002;21:646–652.
9. Richard J C, Pouzot C, Gros A et al. Electrical impedance tomography compared to positron emission tomography for the measurement of regional lung ventilation: an experimental study. *Crit Care*. 2009;13:R82.
10. Ferrario D, Grychtol B, Adler A et al. Toward Morphological Thoracic EIT: Major Signal Sources Correspond to Respective Organ Locations in CT. *IEEE transactions on bio-medical engineering*. 2012;59:3000-8.
11. Frerichs I, Pulletz S, Elke G et al. Assessment of changes in distribution of lung perfusion by electrical impedance tomography. *Respiration*. 2009;77:282-291.
12. The MathWorks Inc. *MATLAB® and Statistics and Machine Learning Toolbox™ Release (R2020a)*. 2020.

Corresponding author:

Author: Arthur Souza Ribeiro
 Institute: Federal University of São Paulo (UNIFESP)
 Street: Av. Vinte e Três de Dezembro, 150
 Jardim das Cerejeiras CEP: 12225-480
 City: São José dos Campos/SP
 Country: Brazil
 Email: arthur.souza@unifesp.br